The Molecular Binding Interactions of Inhibitors and Activators of Phosphoenolpyruvate Carboxylase

Ricardo L. Mancera*[a] and Benjamin J. Carrington[b]

a   Western Australian Biomedical Research Institute, School of Biomedical Sciences and School of Pharmacy, Curtin University of Technology, GPO Box U1987, Perth WA 6845, Australa b Department of Pharmacology, University of Cambridge, Tennis Court Road, Cambridge CB2 1EJ, UK

* Corresponding author. Tel.: +61 8 9266 1017; fax: +61 8 9266 2342; e-mail: r.mancera@curtin.edu.au

Abstract

We have performed molecular modeling studies of the binding to maize phosphoenolpyruvate carboxylase of phosphoenolpyruvate and a number of representative competitive inhibitors. It was found that all these compounds share a common binding mode and that the differences in inhibitory activity of the various inhibitors arise mainly from either increased hydrophobic interactions of *cis* substituents or small but significant changes in their binding mode arising from steric clashes of *trans* substituents with the active site. We have also performed molecular modelling studies of glucose-6-phosphate and a number of other allosteric activators in their putative allosteric binding site in this enzyme. These molecules share the same binding mode for their phosphate moiety while some of them engage in a variety of hydrogen bonding interactions with residues from different subunits of the enzyme, and others establish hydrophobic and van der Waals interactions with other regions of the allosteric binding site.

1. Introduction

Phosphoenolpyruvate carboxylase (PEPC; EC 4.1.1.31) is an enzyme that catalyzes the highly exergonic and irreversible β-carboxylation of phosphoenolpyruvate (PEP) to form oxaloacetate and inorganic phosphate in the presence of Mg^{2+} or Mn^{2+} as a cofactor [1-3]. This enzyme has primarily an anaplerotic role by replenishing C_4-dicarboxylic acids for both energy and biosynthetic metabolisms. In the case of C_4 plants such as maize, the reaction catalyzed by PEPC constitutes the first step in the assimilation pathway of atmospheric CO_2.

Several competitive inhibitors of PEPC that are structural analogs of PEP have been used to try to elucidate the kinetic mechanism of this enzyme and the properties of its active site [2-12]. However, the detailed mechanism of reaction of PEPC, involving PEP, Mg^{2+} (or Mn^{2+}) and HCO_3^-, has not yet been established unambiguously [1-3,13-22].

PEPC is subject to allosteric regulation by various metabolites. The enzyme is activated by D-glucose-6-phosphate (G6P) and inhibited by L-malate and L-aspartate (L-Asp) [2,3,23-26].

Furthermore, the PEPC isoform involved in C_4 photosynthesis by C_4 monocots such as *Z. mays* is also activated by glycine, alanine and serine [21,24,28-33]. All of these groups of regulators are in fact believed to have separate binding sites on the enzyme [9,32,34]. The allosteric G6P binding site [34] can also bind a large number of hexose and triose phosphates as well as other phosphate esters [16,30,32,35-43]. PEP itself can bind to the G6P binding site, thus behaving as both substrate and allosteric activator of PEPC, although this activating effect seems to be due exclusively to the kinetic mechanism of reaction [16,19].

In recent years the X-ray crystal structures of the bacterial (*E. coli*) and the maize (*Z. mays*) forms of PEPC have been reported [44-46]. The overall structure of PEPC was described as being a tetramer of four identical subunits arranged as a "dimer of dimers", with a salt bridge between Arg 438 and Glu 433 in *E. coli* PEPC (Arg 498 and Glu 493 in *Z. mays* PEPC) being responsible for the interaction between the dimmers [44-48]. Each monomeric subunit is made up of an eight-stranded β-barrel and approximately forty α-helices.

The crystal structures of *E. coli* PEPC (EcPEPC) had L-Asp bound to what is believed to be its allosteric binding site [44,47,48]. It was thus thought that the enzyme was in its inactive state (T state). The binding site of L-Asp was found to be located approximately 20 Å away from the active site. One of the four residues involved in the binding of L-Asp is Arg 587, which is part of a conserved glycine-rich loop essential for the catalytic activity of the enzyme. The crystal structures suggest that L-Asp causes the inhibition of PEPC by shifting this glycine-rich loop and another mobile loop away from the active site, with the formation of an ion pair between the sidechain of Arg 587 and the carboxyl group of L-Asp [44,47,48].

The crystal structures of EcPEPC also revealed the likely position of the active site. Mn^{2+} was found bound to the carboxylate sidechain oxygens of Glu 506 and Asp 543 at the C-terminal end of β5 and β6 strands at the top of the α/β barrel of the enzyme [45,47,48]. The coordination sphere of Mn^{2+} was seen to be approximately octahedral, with four water molecules presumably completing the coordination. After soaking the L-Asp-bound EcPEPC crystal with a solution containing Mn^{2+} and the substrate analog 3,3-dichloro-2-dihydroxy-phosphinoylmethyl-2-propenoate (DCDP), the likely binding mode of this PEP analog was also determined [45,47,48]. The phosphate group of DCDP interacts with Mn^{2+}, Arg 396, Arg 699 and Arg 713, all of which presumably stabilize the negative charge of the phosphate group to facilitate the nucleophilic attack by bicarbonate to form carboxyphosphate and enolate of pyruvate in the first step in the proposed reaction mechanism of PEPC [46-48]. A number of hydrophobic residues (Trp 248, Leu 504 and Met 538) were found around the

chlorines of DCDP, indicating the presence of a hydrophobic pocket around the binding site of the methylene group of PEP, as suggested earlier [49].

On the other hand, the crystal structure of *Z. mays* PEPC (ZmPEPC) was not bound with L-Asp but with a sulfate anion, which is also an allosteric activator of PEPC [46-48]. Sulfate binds at the dimer interface where two four-α helix bundles are located, in the vicinity of four positively charged residues (Arg 183, Arg 184, Arg 231 and Arg 372). The ion pairing of sulfate with one of these residues, the conserved Arg 372, could be involved in the rearrangement of each bundle. Arg 372 also interacts with the sidechain of Ser 185 in the helix bundle of the neighboring subunit. It was thus concluded that sulfate binds to the allosteric G6P binding site and that the crystal structure was that of the active state (R state) of ZmPEPC [46-48].

A comparison of EcPEPC and ZmPEPC revealed that the binding of sulfate in the absence of bound L-Asp gives rise to movements of two loops [46-48]. In particular, Arg 647 in ZmPEPC (Arg 587 in EcPEPC), which lies within the conserved glycine-rich loop, moves approximately 15 Å toward the active site. Another conserved loop is also rearranged to interact and stabilize the glycine-rich loop conformation. Specifically, the C-terminal carboxyl group of Gly 970 (Gly 883 in EcPEPC) forms a salt bridge with the side chain of Arg 647. The binding of sulfate also induces the movement of the main chain of the loop comprising residues 174 to 184 toward the active site. Upon sulfate binding, a hydrogen bond is made between the backbone carbonyl of Arg 184 and the backbone NH group of Gln 188, making the α7 helix longer at its N terminus than in EcPEPC and leading to a dynamic movement of the loop toward the active site. The side chain of His 177 is seen more than 10 Å away from the active site in the EcPEPC structure, whereas in the ZmPEPC structure it is next to the active site, consistent with its possible role in stabilizing the carboxyphosphate and abstracting a proton from its carboxyl group in the reaction mechanism of PEPC [46-48,50].

The β barrels of ZmPEPC and DCDP-bound EcPEPC that make up the binding site superimpose rather well [46]. The putative binding mode of PEP in the active site of ZmPEPC was thus suggested on the basis of the structure of the complex of EcPEPC, Mn^{2+} and DCDP [46-48]. In this paper we report the results of molecular modeling studies of the binding of PEP and a number of representative PEP-analog competitive inhibitors to ZmPEPC. We also report the molecular modeling of G6P and a number of other allosteric activators of PEPC in the putative allosteric G6P binding site. The interactions of PEP, inhibitors and activators with their binding sites are analyzed in detail.

2. Methods

The X-ray crystal structures of ZmPEPC (PDB code 1jqo) and EcPEPC (PDB codes 1jqn and 1qb4) were used. The EcPEPC structures were only used to inspect the nature of the coordination of Mn^{2+} by water molecules and the carboxylate sidechain oxygens of Glu 506 and Asp 543, with and without the bound DCDP inhibitor. For all modeling studies, hydrogen atoms were added to the crystal structure of ZmPEPC assuming a pH of 7.0 (all arginines were protonated). Chain A in the PDB file of ZmPEPC was chosen for modeling the active site. His 177 was modeled so that the tautomeric form chosen had ND1 carrying the hydrogen atom, while NE2 was unprotonated, consistent with the proposed role of this histidine as a proton acceptor in the reaction mechanism of PEPC [46-48,50].

The molecular modeling studies reported here were carried out using InsightII 2000 (Accelrys), unless otherwise stated. All energy minimizations were performed with the Discover 3 module using the CFF forcefield [51] and were terminated when the energy gradient reached a value of less than 0.0001 kcal/mol/Å. Conformational changes in a few residues, as described below, were implemented using the Biopolymer module, which uses a rotamer library for generating alternative sidechain conformations [52]. For the energy minimizations, only those residues which had at least one atom within a distance of 40.0 Å from any atom of His 177 were considered. This speeded up significantly the calculations without any loss in accuracy. It is important to mention here that the net charge for the whole crystal structure of ZmPEPC (assuming standard pKa values for all sidechains at a pH of 7.0) is around –40, suggesting the absence of several positively charged residues from the missing loops in the crystal structure and making other kinds of calculations (such as those of the binding energies and/or electrostatic solvation energies) highly unreliable. By taking only the above-described portion of the total protein, the net charge was reduced to around –3.

The first step in modeling the binding mode of PEP and its analogs to the active site of ZmPEPC was to determine the position that Mg^{2+} is likely to have when coordinated to Glu 566 and Asp 603. Mg^{2+} prefers to bind with ligands such as carboxylates, phosphates, carbonyls, hydroxyls and water [53]. It is known from quantum chemical calculations of complexes of Mg^{2+} with several organic molecules that the Mg–O bond length ranges from 2.0 to 2.2 Å [54]. However, in magnesium-bound proteins this length may exceed 2.2 Å due to the lower resolution of the crystal structures surveyed. Nonetheless, high-resolution

proteins (R < 2.0 Å) that have binding sites with one to three carboxylate groups coordinating Mg^{2+} usually exhibit an Mg–O distance of less than 2.2 Å [54].

A Mg^{2+} atom was thus placed in the vicinity of OE1 of the carboxylate group of Glu 566 and of OD2 of the carboxylate group of Asp 603. The sidechain of Asp 603 was given a slightly different low energy rotameric state to that found in the crystal structure to allow Mg^{2+} to move closer into the cavity of the active site, as observed when comparing the crystal structures of EcPEPC and DCDP-bound EcPEPC: Mn^{2+} moves, respectively, from a distance of 6.038 Å from the Cα of Glu 506 to a distance of 6.125 Å, and from a distance of 5.298 Å from the Cα of Asp 543 to a distance of 5.706 Å. An energy minimization was then carried out, keeping the entire protein fixed and using harmonic restraints (with force constants of 500 kcal/mol/Å) to maintain the Mg^{2+} atom at approximately 2.2 Å from its coordinating oxygen atoms in the carboxylate groups of the above mentioned sidechains. Additional weaker harmonic constraints were used to direct the Mg^{2+} atom into the cavity of the active site to ensure that a reasonable final structure was obtained.

The resulting Mg^{2+}-bound ZmPEPC was then used to determine the binding mode of PEP by performing extensive docking simulations. For this purpose the ligand-protein docking program EasyDock was used [55]. A bounding simulation box was defined so as to include the whole of the active site residues. Two hundred docking simulations of PEP were performed. These simulations generated 1000+ solutions that were subsequently efficiently reduced in number by taking only those binding modes where PEP exhibited direct electrostatic interactions with Mg^{2+} through both its phosphate and carboxylate groups (consistent with the observed interactions between DCDP and Mn^{2+} in the crystal structure of EcPEPC [46] and the suggested binding mode of PEP in EcPEPC [45]), as well as hydrogen bonding to one or more of the three positively charged groups in the active site (Arg 456, Arg 759, Arg 773). Theoretical calculations have suggested that coordination of Mg^{2+} by more than three carboxylic groups is not thermodynamically favored in low dielectric environments, such as those found in the active sites of enzymes [54]. However, these calculations did not consider phosphate groups as possible ligands for Mg^{2+}. Furthermore, the crystallographic evidence in the case of EcPEPC confirms that Mn^{2+} is tetravalently coordinated by the carboxylate groups of Glu 566 and Asp 603 as well as the carboxylate and phosphate groups of DCDP.

At this stage the sidechain of Arg 759 was given a slightly different low energy rotameric state to that found in the crystal structure to allow it to move in closer to the phosphate group

of PEP, as is seen in EcPEPC. It is also known that Arg 647 plays a crucial role in the mechanism of reaction of PEPC *after* the formation of the intermediate carboxyphosphate [56]. However, the crystal structure of ZmPEPC revealed that the guanidine group of this residue establishes a strong salt bridge with the C-terminal carboxylate group of Gly 970 [46-48], as well as additional hydrogen bonds with Gln 673 and, possibly, Ser 602. It has been suggested that Arg 647 can adopt a different conformation that would allow it to move closer to the phosphate group of PEP [46-48]. However, for the purpose of modeling the initial binding of PEP it was decided not to change the conformation of Arg 647 since no appropriate alternative low energy rotamer was found. As discussed later, this does not seem to have affected the results.

A few of the best binding modes of PEP that were identified after the docking simulations were then subjected to a full energy minimization under the same conditions as described above, keeping the entire protein (including the Mg^{2+}) rigid. The resulting binding modes were then inspected to ensure that the *si* face of PEP faced the cavity around His 177 and Arg 647, consistent with previous studies suggesting that the carboxylation of PEP occurs on its *si* face [57].

A number of PEP analogs known to be competitive inhibitors of PEPC were also modeled in the active site of ZmPEPC. The compounds chosen were *Z*-bromo-phosphoenolpyruvate (*Z*-Br-PEP), 1-hydroxycyclopropanoic acid phosphate (1-HCP), DCDP, *E*-cyano-phosphoenolpyruvate (*E*-CN-PEP) and phosphoenoltiopyruvate (S-PEP) [2]. The structures of these compounds and their inhibition constants (Ki) against ZmPEPC can be seen in Figure 1. These compounds were modeled by modifying the previously optimized structure of PEP in the active site and then proceeding to carry out a full energy minimization as before.

The binding mode of G6P was determined by docking its molecular structure in the putative allosteric G6P binding site where the sulfate anion was determined in chain A of the crystal structured of ZmPEPC. A bounding simulation box of 15.0 Å away from the sulfate anion was defined and, as before, 200 docking simulations of G6P were performed, generating nearly 800 solutions. In order to find the correct binding mode of G6P, the position and orientation of sulfate in the crystal structure was taken as a reference for the position of the phosphate group of G6P. This is consistent with the observation that sulfate anions are often found bound to the protein binding site of phosphoryl groups of phosphorylated compounds [58]. A few of the best binding modes were thus selected on the basis of the proximity of the phosphate group to the sulfate and the number of hydrogen bonds made to other neighboring

groups. A full energy minimization was then carried out as before, by considering only those protein residues that had at least one atom within a distance of 40.0 Å from the sulfate anion. The resulting protein portion was kept rigid throughout the minimization, with the exception of the hydroxyl group of Ser 185, which is the only rotatable hydrogen bonding group in the vicinity of the putative G6P binding site.

A number of allosteric activators of ZmPEPC that are believed to bind to the same binding site as G6P were also modeled. The compounds chosen were fructose-6-phosphate (F6P), phosphomycin [43] (Pmyc, 1R,2S-epoxypropylphosphonic acid), phenylphosphate [16] (ØP) and acetylphosphate [40] (AcP). The structures of these compounds can be seen in Figure 2. These compounds were docked independently under the same conditions as for G6P, with each series of docking simulations generating 1200+ solutions that were subsequently analyzed and energy minimized in the same manner as for G6P.

3. Results and Discussion

3.1 Modeling of PEP and inhibitors in the active site

The modeling of Mg^{2+} yielded a reasonable location for this cation. Its final position in relation to the carboxylate groups of Glu 566 and Asp 603 can be seen in any of the illustrations in Figure 3. The Mg–O bond lengths are 2.22 Å in the case of the OE1 of Glu 566 and 2.28 Å in the case of the OD2 of Asp 603. These values compare favourably with the Mn–O bond lengths observed in EcPEPC: 2.11 Å and 2.16 Å for the carboxylate groups of Glu 506 and Asp 543, respectively. The modeled Mg^{2+} cation lies just above the plane of the carboxylate groups in a position that should be easily accessible to an incoming phosphate group and/or solvent water molecules.

The modeling of PEP and its analogs in the active site of ZmPEPC yielded a common binding mode for all the molecules. Figure 3 shows the modeled binding modes of PEP, *E*-CN-PEP, S-PEP and 1-HCP. It can be seen that all molecules share the same main interactions with the protein: the phosphate and carboxylate groups each interact electrostatically via one of the oxygens with Mg^{2+} (in the case of PEP, the closest Mg–O distance for the phosphate group is 1.97 Å and the closest Mg–O distance for the carboxylate group is 2.11 Å), and one of the other oxygens in the phosphate group forms two ion pairs with the guanidine group of Arg 456 (in the case of PEP, the hydrogen bond distances are 1.81 Å and 2.37 Å). The phosphate group does not form any other ion pairs or hydrogen bonds, although weaker electrostatic

interactions are to be expected with the guanidine groups of Arg 759 and Arg 773 (in the case of PEP, the closest distances to the phosphate group are 3.06 Å and 3.11 Å, respectively). Further movements in the sidechains of these residues could bring their guanidine groups closer; however, this is likely to require some backbone movement. On the other hand, the proposed mechanism of reaction involving the nucleophilic attack of a bicarbonate anion on the phosphate group of PEP is likely to involve the movement of these sidechains as well as Arg 647 and His 177 to stabilize the resulting carboxyphosphate species [46-48]. Furthermore, the binding of bicarbonate itself is known to involve several basic residues in the 761-768 mobile loop at the C-terminal region and bridging above the β barrel [46-48]. This loop could not be resolved in the crystal structure of ZmPEPC (or in that of EcPEPC) [46].

Earlier quantitative structure-activity relationships (QSAR) studies of PEP analogs suggested that a hydrophobic pocket could lie in the vicinity of the *cis* and *trans* substituents [59]. It was also suggested that *cis* substituents bulkier than hydrogen could increase binding to the active site through more favorable van der Waals interactions [59].

A comparative analysis of the binding modes of the PEP analogs provides some further insight into their varying degrees of inhibitory activity that is in agreement with these QSAR studies [59]. The binding modes of *Z*-Br-PEP and DCDP (not shown in Figure 3) are virtually identical to one another and follow closely the binding mode of PEP, revealing that the presence of *cis* substituents as large as Cl or Br can indeed be easily accommodated in the hydrophobic region lined by Trp 288 and Thr 671, increasing the binding interaction with the active site. The binding mode of 1-HCP (which replaces the vinyl group with a cyclopropyl group) also resembles that of the above molecules and PEP, as seen in Figure 3d.

When comparing the binding modes of DCDP and *E*-CN-PEP (see Figure 3b for the latter) it becomes clear that the pocket lined by Glu 566 and Tyr 601 can accommodate a *trans* substituent as large as Cl with a small level of distortion in the PEP analog molecule. However, a CN group is too bulky and the steric repulsion with the active site "pushes" the PEP analog molecule outwards. This explains the significantly reduced inhibitory activity of *E*-CN-PEP (K_i = 1360 nM) compared to DCDP (K_i = 80 nM). Such distinct effects on the inhibitory activity due to *cis* and *trans* substitutions on the vinyl group of PEP had already been suggested in the past [2,8,9].

It has been suggested that any substitution of the oxygen of the phosphate ester (with a methylene or S atom) results in a considerable decrease in the binding strength possibly due to hydrogen bonding between the oxygen and some group on the active site of the enzyme, or possibly to the variations in bond lengths, bond angles and/or electronic structure associated with these substitutions [9,10]. An early QSAR study found a dependence of the inhibition constants of PEP analogs on the interatomic distance between the phosphate and carboxylate groups [59].

In the case of DCDP, the replacement of the phosphate ester oxygen by a methylene group does not alter significantly the required molecular geometry to maintain the direct interactions of the phosphate group with Mg^{2+} and Arg 456. As can be seen in Figure 3c, a replacement by a S atom in S-PEP increases significantly the vinyl–S bond length, translating into the vinyl group being pushed toward Ser 602 and away from the neighboring hydrophobic region (Trp 288 and Thr 671). The interactions of S-PEP with Mg^{2+} and Arg 456 are nonetheless preserved. The reduced inhibitory activity of S-PEP (Ki = 2000 nM) is thus the result, to a significant extent, of this modified binding mode with steric impediments.

We can see that the differences in inhibitory activity of the various PEP analogs arise from either increased hydrophobic interactions of *cis* substituents or changes in the binding mode of their vinyl group arising from steric clashes of *trans* substituents with the active site. However, it is likely that changes in the electronic structure of this molecule also play a major role, particularly in relation to the overall negative charge of the phosphate group, as was observed before [59].

The X-ray determination of the structure of ZmPEPC complexed with a few of the above PEP analog inhibitors would provide confirmation of the coordination structure of Mg^{2+}, the modeled binding modes and any conformational changes that may take place in one or more of the sidechains that make up the active site.

3.2. Modeling of activators in the allosteric G6P binding site

The G6P binding site is a well defined pocket in the vicinity of the sulfate anion in the crystal structure ZmPEPC. This pocket is predominantly hydrophobic, with two main hydrophobic regions: one defined by the sidechains of Phe 328 and Phe 361, and another one defined by Arg 242 (the hydrophobic portion of its sidechain), Ala 239, Tyr 243 and Pro 235. In the crystal structure of ZmPEPC, sulfate interacts directly with the sidechain of Arg 231 (two ion

pairs), the sidechain and backbone of Ser 185 (two hydrogen bonds) and the backbone of Arg 184 (one hydrogen bond). The guanidine group of Arg 183 is approximately 3.5 Å away from the sulfate anion, but it does not have the right orientation to form an ion pair. The guanidine group of Arg 372 is 5 Å away from the sulfate anion and would establish a weak electrostatic interaction. The only other hydrogen bonding groups in the G6P binding site are those afforded by the guanidine group of Arg 184, the sidechain of Glu 360, the backbone of Phe 361 and the backbone and sidechain of Trp 362. Figure 4 illustrates the positions of the active site and the allosteric G6P binding site within a simplified representation of the secondary structural elements of ZmPEPC. The main interacting groups in the G6P binding site can be seen in any of the illustrations in Figure 5.

It is clear that the putative G6P allosteric binding site is capable of accommodating a variety of phosphorylated molecules. In the case of PEP analogs, whether they can bind to this site and act as activators or bind to the active site and act as competitive inhibitors has been suggested to be due to the nature of their complexes with Mg^{2+} [43]. All competitive inhibitors of PEPC are trianionic in nature, while most allosteric activators are dianionic in nature. PEP itself is a notable exception, being trianionic in nature. However, since its activating effect seems to be due exclusively to the kinetic mechanism of reaction [19], the binding of PEP to the G6P allosteric binding site would not trigger an allosteric transition. The degree of activation of the modeled compounds increases along the series Pmyc > G6P > ØP > F6P > AcP [43]. Figure 5 shows the modeled binding modes of the first four activators, and sulfate is shown as reference.

The binding mode of G6P, shown in Figure 5a, is representative of the activators that were modeled. The phosphate group has an optimized position and orientation that is similar to that observed for the sulfate anion, and it is able to establish the same number of ion pairs (two) and hydrogen bonds (three) with the same groups in the binding site. The hexose ring establishes a number of hydrogen bonds: one is made with the backbone NH of Phe 361, another one is made with the carboxylate group of Glu 360 and two more are made with the guanidine group of Arg 184. A further intramolecular hydrogen bond is seen involving the phosphate ester oxygen atom and the closest OH group in the ring. It is likely that further hydrogen bonding interactions are made with solvent water molecules.

F6P has a similar binding mode to that of G6P, as seen in Figure 5c. The phosphate group forms the same ion pairs and hydrogen bonds, and the pentose ring establishes hydrogen bonds with the guanidine group of Arg 184 and the carboxylate group of Glu 360. While no

hydrogen bond is made with the backbone NH of Phe 361 as in the case of G6P, a small conformational change in Trp 362 could provide a further hydrogen bond with the terminal CH_2OH group in F6P, which in the shown binding mode lies at a distance of just under 2.6 Å. F6P is also seen to have an intramolecular hydrogen bond involving the phosphate ester oxygen atom and the closest OH group in the ring.

ØP has a binding mode that reflects the hydrophobic nature of its phenyl ring, as seen in Figure 5e. The phosphate group forms the same ion pairs and hydrogen bonds as with G6P and F6P. A portion of the phenyl ring lies on top of the hydrophobic region of the sidechain of Arg 242, with other portions of the phenyl ring in close proximity to the hydrophobic regions of Pro 235, Ala 239 and Tyr 243.

Pmyc and AcP have a similar binding mode to that of ØP. The binding mode of Pmyc is shown in Figure 5g. Their phosphate groups form the same ion pairs and hydrogen bonds as the previous activators. The hydrophobic epoxy group in Pmyc follows the same geometry as the phosphate ether bridge in the previous activators, lying above the hydrophobic region of the sidechain of Arg 242. The methyl substituent lies in the vicinity of Pro 235. This is also observed with the acetyl group in AcP (not shown).

There are two main features of the binding of allosteric activators to the G6P binding site of ZmPEPC. The first feature concerns the interactions of Arg 372 in subunit B with the phosphate group (through weak ion pairing) and with the hydroxyl group of Ser 185 (through hydrogen bonding) in the helix bundle of subunit A. Both of these interactions appear to be involved in the rearrangement and stability of the α bundles in neighboring subunits [46-48]. The second feature concerns the hydrogen bond seen between the backbone NH of Arg 184 and the carboxylate group of Glu 188. This interaction is believed to be responsible for making the α7 helix longer at its N terminus (compared to that in EcPEPC), which leads to a movement of the loop comprising residues 174 to 184 toward the active site, bringing the catalytically important sidechain of His 177 next to the active site [46-48].

Both G6P and F6P establish hydrogen bonding interactions through their sugar rings that reinforce the interaction between subunits A and B, particularly the ion pair observed between the guanidine group of Arg 184 in subunit A and the carboxylate group of Glu 360 in subunit B. As mentioned above and as shown in Figures 3a and 3c, G6P and F6P each form two hydrogen bonds with Arg 184 and one hydrogen bond with Glu 360. G6P forms an additional hydrogen bond with the backbone NH of Phe 361 in subunit B while F6P could form an

additional hydrogen bond with the sidechain of Trp 362 (also in subunit B) after a small conformational change. Since the conformation of the sidechain of Arg 184 is that one already observed in the crystal structure of ZmPEPC with bound sulfate, it is thus likely that the interactions with the sugar rings of either G6P or F6P help to stabilize the local conformation of the allosteric binding site in the activated R state of the enzyme.

ØP, Pmyc and AcP all lack the above interactions with residues from subunit B. However, all of the five allosteric activators considered have direct van der Waals (and hydrophobic) interactions with various residues in subunit A, in particular with Arg 242 and Pro 235. In addition, ØP has van der Waals contacts with Ala 239 and Tyr 243. Figure 5 also highlights the portions of those secondary structural elements that have atoms within van der Waals distance (< 3.5 Å) of each one of the modeled activators. It is possible that these interactions further stabilize the observed conformation of the active site through inter-loop interactions.

It is possible that the allosteric activators exhibit varying degrees of activation as a consequence of the proposed distinct nature of their interactions upon binding (see Figure 4). While the binding of their phosphate groups is essential for their activating effect on ZmPEPC, the remaining interactions with the allosteric binding site may contribute to optimizing the structure of the R state of the enzyme. In particular, the effect in different activators of phosphate binding to the conformation of the α7 helix and, consequently, the 174-184 loop that is involved in the active site remains to be investigated. Inter-loop interactions may also play a role in optimizing the geometry of the active site for different allosteric activators, particularly in view of the different interactions that these ligands have with the α9 helix and the subsequent loop. Further molecular modeling studies involving an analysis of ligand-induced changes in the flexibility of the enzyme are likely to provide further insight into the differences between various allosteric activators.

4. Conclusions

We have performed molecular modeling studies of the binding to ZmPEPC of PEP and a number of representative PEP analog competitive inhibitors. The studies suggest that the binding mode of PEP and its analogs involves the electrostatic interaction of both the phosphate and carboxylate groups with the Mg^{2+} cation (which is in turn coordinated to Glu 566, Asp 603 and most likely one or possibly two water molecules in the binding site). These compounds were determined to share a common binding mode and the differences in

inhibitory activity of the various inhibitors arise mainly from either increased hydrophobic interactions of *cis* substituents or small but significant changes in their binding mode arising from steric clashes of *trans* substituents with the active site.

We have also performed molecular modeling studies of G6P and a number of other allosteric activators in the putative allosteric G6P binding site in ZmPEPC. We have determined that these molecules share a common binding mode for their phosphate moiety while some of them (G6P and F6P) engage in a variety of hydrogen bonding interactions with residues from different subunits of the enzyme, and others (ØP, Pmyc and AcP) establish hydrophobic and van der Waals interactions with different regions of the allosteric binding site. These distinct interactions are likely to be involved in stabilizing the local conformation of the allosteric binding site in the R state of the enzyme and the conformation of the mobile loop containing His 177 involved in the active site.

Acknowledgements

References

1. O'Leary, M.H., Ann. Rev. Plant Physiol, 33 (1982) 297

2. Andreo, C.S., González, D.H., and Iglesias, A.A., FEBS Lett., 213 (1987) 1.

3. Chollet, R., Vidal, J., and O'Leary, M.H., Ann. Rev. Plant Physiol. Plant Mol. Biol., 47 (1996) 273.

4. González, D.H., Iglesias, A.A., and Andreo, C.S., Arch. Biochem. Biophys., 245 (1986) 179.

5. Iglesias, A.A., González, D.H., and Andreo, C.S., Biochim. Biophys. Acta, 788 (1984) 41.

6. Stiborová, M., and Leblová, S., Physiol. Veg., 21 (1983) 935.

7. Iglesias, A.A., and Andreo, C.S., Biochim. Biophys. Acta, 749 (1983) 9.

8. González, D.H., and Andreo, C.S., Trends Biochem. Sci., 14 (1989) 24.

9.   O'Leary, M.H., Physiol. Veg., 21 (1983) 88.

10.   Sikkema, K.D., and O'Leary, M.H., Biochemistry, 27 (1988) 134.

11.   Liu, J., Peliska, J.A., and O'Leary, M.H., Arch. Biochem. Biophys., 277 (1990) 143.

12.   García-Alles, L.F., and Erni, B., Eur. J. Biochem., 269 (2002) 3226.

13.   Miller, R.S., and Lane, M.D., J. Biol. Chem., 22 (1968) 6041.

14.   Mukerji, S.K., Arch. Biochem. Biophys., 182 (1977) 352.

15.   Wedding, R.T., Rustin, P., Meyer, C.R., and Black, M.K., Plant Physiol., 88 (1988) 976.

16.   Rodríguez-Sotres, R., and Muñoz-Clares, R.A., Arch. Biochem. Biophys., 276 (1990) 180.

17.   Janc, J.W., O'Leary, M.H., and Cleland, W.W., Biochemistry, 31 (1992) 6421.

18.   Lepiniec, L., Vidal, J., Chollet, R., Gadal, P, and Cretin, C., Plant Sci., 99 (1994) 111.

19.   Tovar-Méndez, A., Rodríguez-Sotres, R., López-Valentín, D.M., and Muñoz-Clares, R.A., Biochem. J., 332 (1998) 633.

20.   Frank, J., Vater, J., and Holzwarth, J.F., Phys. Chem. Chem. Phys., 1 (1999) 455.

21.   Tovar-Méndez, A., Mújica-Jiménez, C., and Muñoz-Clares, R.A., Plant Physiol., 123 (2000) 149.

22.   Tovar-Méndez, A., and Muñoz-Clares, R.A., Biochim. Biophys. Acta, 1546 (2001) 242.

23.   Coombs, J., Baldry, C.W., and Bucke, C., Planta, 110 (1973) 95.

24.   Stiborová, M., and Leblová, S., Photosynthetica, 19 (1985) 177.

25.   Frank, J., Clarke, R.J., Vater, J., and Holzwarth, J.F., Biophys. Chem., 92 (2001) 53.

26.   Huber, S.C., and Edward, G.E., Can J. Bot., 53 (1975) 1925.

27.   Vidal, J., and Chollet, R., Trends Plant Sci., 2 (1997) 230.

28.   Nishikido, T., and Takanashi, H., Biochem. Biophys. Res. Commun., 53 (1973) 126.

29.   Uedan, K., and Sugiyama, T., Plant. Physiol., 57 (1976) 906.

30.   Doncaster, H.D., and Leegood, R.C., Plant Physiol., 84 (1987) 82.

31. Garson, L., and Gray, V., Biochem. Int., 23 (1991) 299.

32. Bandarian, V., Poehner, W.J., and Grover, S.D., Plant Physiol., 100 (1992) 1411.

33. Gillinta, J., and Grover, S.D., Photosynth. Res., 45 (1995) 121.

34. Tovar-Méndez, A., Mújica-Jiménez, C., and Muñoz-Clares, R.A., Biochim. Biophys. Acta, 1337 (1997) 207.

35. Mukerji, S.K., Arch. Biochem. Biophys., 182 (1977) 360.

36. Lavergne, D., and Champigny, M.-L., Physiol. Veg., 21 (1983) 1021.

37. Selinioti, E., Karabourniotis, G., Manetas, Y., and Gavalas, N.A., J. Plant Physiol., 121 (1985) 353.

38. Stiborová, M., and Leblová, S., FEBS Lett., 205 (1985) 32.

39. Jenkins, C.L.D., Harris, R.L.N., and McFadden, H.G., Biochem. Int., 12 (1986) 619.

40. González, D.H., Iglesias, A.A., and Andreo, C.S., Biochem. J., 241 (1987) 543.

41. Peliska, J.M., and O'Leary, M.H., Biochemistry, 28 (1989) 1604.

42. Tovar-Méndez, A., Yampara-Iquise, H., Mújica-Jiménez, C., and Muñoz-Clares, R.A., (Mathis, P., Ed.), Photosynthesis: from Light to Biosphere - Proceedings of the Xth International Photosynthesis Congress, Montpellier, France, August 20–25, 1995, Kluwer, Dordrecht., 1995, pp 155-158.

43. Mújica-Jiménez, C., Castellanos-Martínez, A, and Muñoz-Clares, R.A., Biochim. Biophys. Acta, 1386 (1998) 132.

44. Kai, Y., Matsumura, H., Inoue, T., Terada, K., Nagara, Y., Yoshinaga, T., Kihara, A., Tsumura, K., and Izui, K., Proc. Natl. Acad. Sci. USA, 96 (1999).

45. Matsumura, H., Terada, M., Shirakata, S., Inoue, T., Yoshinaga, T., Izui, K., and Kai, Y., FEBS Lett., 458 (1999) 93.

46. Matsumura, H., Xie, Y., Shirakata, S., Inoue, T., Yoshinaga, T., Ueno, Y., Izui, K., and Kai, Y., Structure, 10 (2002) 1721.

47. Kai, Y., Matsumura, H., and Izui, K., Arch. Biochem. Biophys., 414 (2003) 170.

48. Izui, K., Matsumura, H., Furumoto, T., and Kai, Y., Annu. Rev. Plant. Biol., 55 (2004) 69.

49. Izui, K., Matsuda, Y., Kameshita, I., Katsuki, H., and Wood, A.E., J. Biochem., 94 (1983) 1789.

50. Terada, K., and Izui, K., Eur. J. Biochem., 202 (1991) 797.

51. Dinur, U., and Hagler, A.T., (Lipkowitz, K.B., and Boyd, D.B., Eds.) Approaches to empirical force fields, in Reviews in Computational Chemistry, Vol. 2, VCH Publishers, New York, 1991, pp. 99-164

52. Ponder, J.W., and Richards, F.M., J. Mol. Biol., 193 (1987) 775.

53. Burgess, M.A., Metal ions in solution, Ellis Horwood, Chichester, UK, 1978.

54. Dudev, T., Cowan, J.A., and Lim, C., J. Am. Chem. Soc., 121 (1999) 7665.

55. Mancera, R.L., Källblad, P., and Todorov, N.P., J. Comput. Chem., 25 (2004) 858.

56. Yano, M., Terada, K., Umiji, K., and Izui, K., J. Biochem. (Tokyo), 117 (1995) 1196.

57. Rose, I.A., O'Connell, E.L., Noce, P., Utter, M.F., Wood, H.G., Cooper, T.G., and Benziman, M., J. Biol. Chem., 244 (1969) 6130.

58. Pai, E.F., Sachsenheimer, W., Schirmer, R.H., and Schulz, G.E., J. Mol. Biol., 114 (1977) 37.

59. Mancera, R.L., Gómez, A.G., and Pisanty, A., Bioorg. Med. Chem., 3 (1995) 217.

Figure captions

Figure 1. Chemical structures and inhibition constants of several competitive inhibitors of ZmPEPC.

Figure 2. Chemical structures of several allosteric activators of ZmPEPC.

Figure 3. Modeled binding modes of phosphoenolpyruvate and several competitive inhibitors in the active site of ZmPEPC. The modeled Mg^{2+} is shown as a purple sphere, and all relevant hydrogen bonds/electrostatic interactions are highlighted with narrow lines. (a) PEP, (b) *E*-CN-PEP, (c) S-PEP, and (d) 1-HCP. All figures were produced using Insight 2000 (Accelrys).

Figure 4. Positions of the active site and the allosteric G6P binding site within a simplified representation of the secondary structural elements of ZmPEPC. Both PEP (with Mg^{2+}) and G6P are shown in their modeled binding modes. The location and connectivity of the 174-184 loop and the α7 helix are also highlighted. β-sheets are shown in yellow, α-helices are shown in red, loops are shown in pink and β–turns are shown in blue. Some of the relevant sidechains in both binding sites are shown explicitly in sticks, while Mg^{2+} is shown as a purple sphere. This figure was produced using Insight 2000 (Accelrys).

Figure 5. Modeled binding modes of several allosteric activators in the putative glucose-6-phosphate allosteric binding site of ZmPEPC. The crystallographic position of sulfate (colored in cyan) is shown as reference, and all relevant hydrogen bonds/electrostatic interactions are highlighted with narrow lines. In the secondary structure representation of the protein, those regions that make direct van der Waals interactions with the bound ligand are colored in purple, while the ligands are shown with a CPK representation. (a) Atomic representation of the binding mode of G6P, (b) Secondary structure representation of the binding mode of G6P, (c) Atomic representation of the binding mode of F6P, (d) Secondary structure representation of the binding mode of F6P, (e) Atomic representation of the binding mode of ØP, (f) Secondary structure representation of the binding mode of ØP, (g) Atomic representation of the binding mode of Pmyc, and (h) Secondary structure representation of the binding mode of Pmyc. All figures were produced using Insight 2000 (Accelrys).

Figure 1
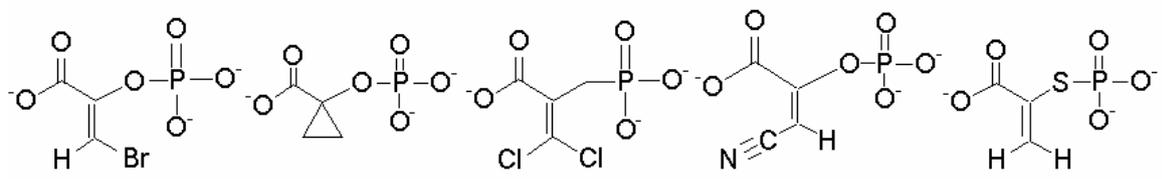
Z-Br-PEPC	1-HCP	DCDP	E-CN-PEP	S-PEP
(Ki = 7 µM)	(Ki = 7 µM)	(Ki = 80 µM)	(Ki = 1360 µM)	(Ki = 2000 µM)
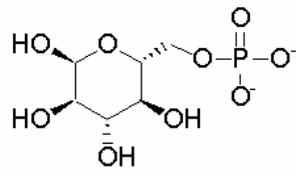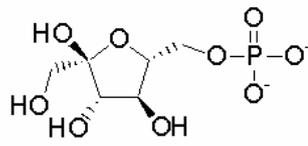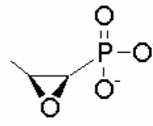
Figure 2
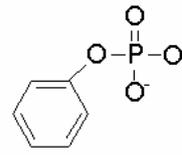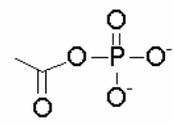
G6P   F6P   Pmyc   ØP   AcP

Figure 3

Figure 4

Figure 5